# A New Nanosecond UV Laser at 355 nm: Early Results of Corneal Flap Cutting in a Rabbit Model

Andrea Trost,[1] Falk Schrödl,[1,2] Clemens Strohmaier,[1] Barbara Bogner,[1] Christian Runge,[1] Alexandra Kaser-Eichberger,[1] Karolina Krefft,[1] Alfred Vogel,[3] Norbert Linz,[3] Sebastian Freidank,[3] Andrea Hilpert,[4] Inge Zimmermann,[4] Günther Grabner,[1] and Herbert A. Reitsamer[1]

[1]Department of Ophthalmology, SALK/University Clinic, Paracelsus Medical University, Salzburg, Austria
[2]Department of Anatomy, Paracelsus Medical University, Salzburg, Austria
[3]Institute of Biomedical Optics, University of Lübeck, Lübeck, Germany
[4]Department of Anatomy I, University Erlangen–Nuremberg, Erlangen, Germany

Correspondence: Herbert A. Reitsamer, Department of Ophthalmology, SALK Muellner Hauptstrasse 48, 5020 Salzburg, Austria; h.reitsamer@salk.at.

AT and FS contributed equally to the work presented here and should therefore be regarded as equivalent authors.

Submitted: June 11, 2013
Accepted: August 19, 2013

Citation: Trost A, Schrödl F, Strohmaier C, et al. A new nanosecond UV laser at 350 nm: early results of corneal flap cutting in a rabbit model. *Invest Ophthalmol Vis Sci*. 2013;54:7854–7864. DOI:10.1167/iovs.13-12580

**Purpose.** A new 355 nm UV laser was used for corneal flap cutting in an animal model and tested for clinical and morphologic alterations.

**Methods.** Corneal flaps were created (Chinchilla Bastards; $n = 25$) with an UV nanosecond laser at 355 nm (150 kHz, pulse duration 850 ps, spot-size 1 μm, spot spacing 6 × 6 μm, side cut Δz 1 μm; cutting depth 130 μm) and pulse energies of 2.2 or 2.5 μJ, respectively. Following slit-lamp examination, animals were killed at 6, 12, and 24 hours after treatment. Corneas were prepared for histology (hematoxylin and eosin [HE], TUNEL-assay) and evaluated statistically, followed by ultrastructural investigations.

**Results.** Laser treatment was tolerated well, flap lift was easier at 2.5 μJ compared with 2.2 μJ. Standard HE at 24 hours revealed intact epithelium in the horizontal cut, with similar increase in corneal thickness at both energies. Irrespective of energy levels, TUNEL assay revealed comparable numbers of apoptotic cells in the horizontal and vertical cut at 6, 12, and 24 hours, becoming detectable in the horizontal cut as an acellular stromal band at 24 hours. Ultrastructural analysis revealed regular morphology in the epi- and endothelium, while in the stroma, disorganized collagen lamellae were detectable representing the horizontal cut, again irrespective of energy levels applied.

**Conclusions.** This new UV laser revealed no epi- nor endothelial damage at energies feasible for corneal flap cutting. Observed corneal swelling was lower compared with existing UV laser studies, albeit total energy applied here was much higher. Observed loss of stromal keratinocytes is comparable with available laser systems. Therefore, this new laser is suitable for refractive surgery, awaiting its test in a chronic environment.

Keywords: nanosecond UV laser, corneal, histology, rabbit, refractive surgery

In refractive surgery, LASIK is currently the most commonly used technique to change the shape of the corneal stroma. Here, access to the stroma is achieved by removing the epithelium and adjacent superficial stromal layers by means of a cut that creates a corneal flap.[1] The refractive correction is then performed using ArF excimer laser pulses operating in the UV range at the 193 nm wavelength.[2] Flap cutting was originally performed with the aid of a microkeratome, but better reproducibility and the option of performing vertical side cuts were gained when femtosecond lasers were introduced for this procedure in the early 21st century.[3,4] These lasers usually operate in the infrared range at wavelengths between 1030 and 1053 nm, and the laser energy applied leads to the separation of the stromal lamellae via photodisruption[5] (i.e., focal plasma spots generate cavitation bubbles that separate stromal lamellae while expanding).

However, the cutting precision of lasers in the infrared range has inherent physical limits due to the long wavelength. Changing the wavelength of the laser source to the UV range results both in a smaller diameter and in a shorter length of the laser focus. Consequently, improved precision of flap shaping can be expected taking the achievable quality of refractive surgery in the cornea to a new level.

Recently, Vogel et al.[6] introduced an UV laser operating at 355 nm for flap creation, with a pulse duration in the nanosecond range. This new laser might be able to increase the precision of flap creation as described above and an additional cooling system is not required.[7] A further advantage is the microchip-based control element, which leads to a compact and cost effective UV laser tool.[6,7]

However, three major questions need to be addressed when operating in the cornea with a laser source in the UV range. Firstly, regarding flap formation, which pulse energies are needed for a reliable flap formation? Secondly, regarding UV light, is the laser source safe, that is, does the energy dose required for flap cutting remain below the photochemical damage threshold? Thirdly, regarding the photodisruptive physical laser effects, are the thermomechanical effects of shock wave emission and cavitation induced by the plasma formation tolerable in the treated tissue?

To address these questions, we tested the new nanosecond laser in a rabbit model using different laser energies at 6 × 6 μm

**Table 1.** Groups and Experimental Procedure

| Pulse Energy | Spot Distance | Dose | Cut Depth | Time Point | # Rabbits | Analysis |
|---|---|---|---|---|---|---|
| 2.2 μJ | 6 × 6 μm | 6.1 J/cm² | 130 μm | Acute | 1 | Flap lift |
| 2.2 μJ | 6 × 6 μm | 6.1 J/cm² | 130 μm | 6 h | 6 | Morphologic analysis |
| 2.2 μJ | 6 × 6 μm | 6.1 J/cm² | 130 μm | 12 h | 6 | HE staining, TEM, TUNEL, corneal thickness |
| 2.2 μJ | 6 × 6 μm | 6.1 J/cm² | 130 μm | 24 h | 6 | Clinical evaluation |
| 2.5 μJ | 6 × 6 μm | 6.9 J/cm² | 130 μm | 24 h | 5 | Photodocumentation, slit-lamp examination |
| 2.5 μJ | 6 × 6 μm | 6.9 J/cm² | 130 μm | Acute | 1 | Flap lift |

spot separations to characterize the flap formation and to address the question of thermal or photochemical damage on corneal tissue.

## Materials and Methods

### Anesthesia and Animal Treatment

All animal procedures were performed in accordance with the ARVO regulations for Animal Use in Ophthalmic and Vision Research. Pigmented rabbits (Chinchilla Bastard; $n = 25$; Charles River, Kisslegg, Germany) were anesthetized with a combination of ketamine/xylazine (40 mg/kg, i.m.; 5 mg/kg, intramuscular [i.m.], respectively; Pfizer, Vienna, Austria/ Sigma-Aldrich, Vienna, Austria), and pCO2, and heart rates were monitored (Capnograph, V90041; Surgi Vet, Waukesha, WI). To avoid irritation of the corneal surface, topical anesthesia (0.4% Novain; AGEPHA GmbH, Vienna, Austria) was applied prior to any manipulation, followed by topical application of tropicamid 0.5% and phenylephrin 2.5%. Eyes were disinfected using polyvidon-iodide eye drops (Betaisodona 5%; Mundipharma, Vienna, Austria), followed by a triple rinse with physiological saline solution (0.9%). Left eyes were treated while right eyes served as untreated controls. Animals were allowed to survive 24 hours and were killed by an overdose of thiopental.

### Laser Parameters

Corneal flaps were created (depth 130 μm) with the UV nanosecond laser (Schwind eye-tech-solutions, Kleinostheim, Germany) at a wavelength of 355 nm. Two different pulse energies were set at 2.2 and 2.5 μJ. In all experiments, pulse frequency was 150 kHz, pulse duration 850 ps, spot size 1 μm, spot spacing 6 × 6 μm, and side cut Δz 1 μm. The total UV dose employed in flap cutting was 6.1 and 6.9 J/cm², respectively, for the horizontal cuts. To create a flap of 6.5 mm in diameter a customized, multiuse application interface of stainless steel combined with disposable glass slides (silica glass, transmission > 92% at 355 nm, diameter 12.7 mm, thickness 1 mm) was used. Flaps were kept in place for subsequent analysis. Two rabbits received laser treatment on both eyes with the different pulse energies and those were used to proof the feasibility of lifting the flap, but received no further analysis. A detailed list of experimental groups and procedures is given in Table 1.

Photodocumentation of the eyes and corneal surface (Axiocam; Zeiss, Oberkochen, Germany) was carried out immediately after laser treatment and at 24-hours posttreatment.

### Morphologic Analysis and Documentation

Eyes were removed 6-, 12-, and 24-hours posttreatment and fixed via immersion in phosphate buffer containing 4% paraformaldehyde (PFA) and embedded in paraffin. Eyes were further processed for standard hematoxylin-eosin staining (HE staining) of 3-μm slices and slides were photodocumented via an inverted light-microscope (Observer Z.1; Zeiss) equipped with a digital camera (Axiocam HRC; Zeiss).

For ultrastructural analysis, corneal halves were fixed in 4% PFA containing 1.5% glutaraldehyde (Sigma-Aldrich), postfixed in 1% osmium tetroxide, dehydrated through graded alcohols, embedded in Epon, and mounted on Epon blocks. Semithin sections were stained with methylene blue. Silver-grey serial ultrathin sections were lightly contrasted with lead citrate and examined with the transmission electron microscope (TEM; Leo906; Zeiss).

### TUNEL Assay

To detect the amount of apoptotic/necrotic cells at the different laser pulse energies used, TUNEL assay (DeadEnd Flurometric Apoptosis Detection System G3250; Promega, Mannheim, Germany) was performed on 3-μm paraffin sections after laser treatment. This assay is based on the catalytically incorporation of fluorescein-12-dUTP at 3′-OH DNA ends by the recombinant terminal deoxynucleotidyl transferase (rTdT). The enzyme rTdT forms a polymeric tail that can be visualized by fluorescence microscopy showing the damaged nuclei in green. Positive controls were treated with DNAseI to induce double strand breaks and resulted in bright green fluorescence, while negative controls were processed lacking rTdT in the incubation and resulted in no staining. To evaluate the corneal cell density, sections were counterstained with 4′,6-diamidino-2-phenylindole dihydrochloride (DAPI), resulting in blue nuclear staining. In order to document TUNEL results, a confocal laser scanning unit (LSM710 attached to Axio ObserverZ1; ×20 dry or ×40 and ×60 oil immersion objective lenses, with numeric apertures 0.8, 1.30, and 1.4, respectively; Zeiss) was used. Sections were imaged using the appropriate filter settings for fluorescein (495 nm excitation, channel 1, coded green) and DAPI (350 nm excitation, channel 2, coded blue).

### Measurement of Corneal Thickness

In addition to the clinical evaluation and TUNEL assays of the corneal epithelium, corneal edematous swelling as a symptom of photokeratitis immediately after UV laser light exposure was quantified with measurements of corneal thickness on histologic slides 24 hours after laser treatment. For that, total corneal thickness (i.e., distance from the superficial epithelial layer to the inner border of endothelium) was measured in the horizontal cut region (Axio ObserverZ1 attached to LSM710; Zeiss) and compared with the adjacent untreated region in the same eye. The comparison of central versus peripheral cornea is applicable because, in rabbits, central and peripheral corneal thickness shows no difference.[8,9]

Investigative Ophthalmology & Visual Science

### Measurement of Corneal UV Transmittance During Flap Cutting

Corneal UV transmittance during flap cutting at 355 nm was determined in initial experiments on freshly obtained porcine cadaver corneas to assess the UV dose reaching the endothelium. Flaps were created with different laser pulse energies using a microchip laser (μFlare, 10 kHz repetition rate, 400 ps pulse duration, 355 nm wavelength, NA 0.34; Innolight GmbH, Hannover, Germany). The transmitted UV light, after passing the cornea, was detected with a power meter (Ophir PD 300-UV; Ophir Optronics Solutions Ltd., Jerusalem, Israel) and compared with the incident laser pulse energy.

### Cell Counts and Statistical Analysis

When further investigating the horizontal cut, nuclear DAPI staining, and subsequent fluorescence microscopy facilitated detection of this region compared with HE staining. The cut appeared as hypocellular belt-like area surrounded by DAPI-positive nuclei of stromal keratinozytes. This technique was therefore chosen for further quantification.

Out of the TUNEL-stained corneal sections, three non-neighbored slides of each cornea displaying the horizontal cut were selected and automatically analyzed for the number of TUNEL-positive cells compared with the number of DAPI-positive keratinocytes. A region of interest (ROI) was defined covering the corneal stroma region (from border epithelium to border endothelium) in these slides, and the portion of apoptotic and necrotic cells in the ROI was assessed.

For that purpose, single confocal optical sections of both channels were converted into grey scale images and imported into ImageJ software (available in the public domain, http://rsb.info.nih.gov; National Institutes of Health, Bethesda, MD). Quantitative evaluation was performed using ITCN 1.6, a plugin for the Image software (available in the public domain, http://rsb.info.nih.gov/ij/plugins/itcn.html) designed for automatic cell counting. While actual cell counts were performed via ITCN, each analyzed image was also manually checked for adequate cell detection parameters. The vertical cut at the margin of the flap is exposed to maximum laser dose, whereas the horizontal cut creating the flap bed obviously received a lower laser dose.

Statistical analysis was performed with Sigmastat 12 (Systat GmbH, Erkrath, Germany). Differences between experimental groups were assessed with ANOVA and subsequent post hoc *t*-tests with Bonferroni correction. *P* values less than 0.05 were considered statistically significant.

## Results

### Clinical Evaluation

The laser treatment was well tolerated in all animals investigated. Immediately after laser treatment, a uniform bubble layer in the cornea with a well-defined peripheral cutting edge was visible. The bubble layer disappeared gradually, and after 30 minutes the bubbles vanished (Figs. 1A, 1D). Following the laser treatment, a minor conjunctival irritation was detectable in four animals, as well as a low-grade photophobia in six animals, however, those symptoms disappeared within a few hours. All of the animals showed regular behavior and normal food intake after laser treatment. No corneal infections or opacities were observed. Clinically and macroscopically, no kind of abnormalities were detectable, nor were any other complications observed during the period investigated (Figs. 1B, 1E). Retrograde illumination after 24 hours revealed a ring-like structure in the corneal surface reflecting the vertical laser cut (Figs. 1C, 1F). No biomicroscopic difference between the two applied laser energies was detected.

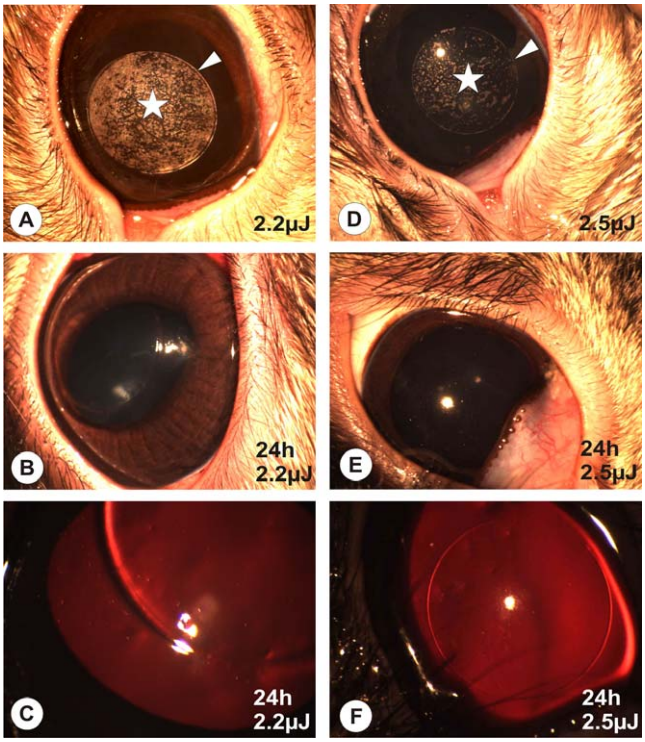


**Figure 1.** Photomicrograph of the ocular surface after flap dissection with two different laser energies (2.2 μJ, [**A–C**]; 2.5 μJ, [**D–F**]). Directly after laser application (**A**, **D**), the vertical cut (*arrowhead*) and adjacent "bubble layer" of the horizontal cut (*asterisk*) are clearly visible. Twenty-four hours after treatment, the corneal surface appears intact without opacity (**B**, **E**) and this finding is confirmed in retrograde illumination (**C**, **F**). No difference between the effects produced by the different pulse energies was detectable.

### Lifting the Flap

A flap lift was performed in four eyes out of two animals that had been treated with the different laser energies of 2.2 and 2.5 μJ. A pulse energy of 2.2 μJ allowed for an easy detachment of the corneal flap, with a homogenous stromal bed remaining (Figs. 2A, 2B). An increase of the cutting energy to 2.5 μJ further facilitated the flap detachment and opening of the stromal bed (Figs. 2C, 2D). Flap-lifted corneas were not subjected to any further analysis.

### Standard Histology

Hematoxylin and eosin staining 24 hours after laser treatment revealed an intact epithelial layer with epithelial dip in the region of the side cut. For both laser energies this epithelial dip reached into the superficial quarter of the stroma. The dip was filled with regular epithelial cells and the border between epithelium and stroma was intact (Figs. 3A, 3C). Stromal collagen lamellae lined the dip to the lower margin of the vertical cut. Here, remnants of stromal keratinocytes were detectable at 2.2-μJ energy, while at 2.5 μJ an edematous zone of 20 × 20 μm without any cells was detectable. This zone reached down into the middle of the stroma with continuously decreasing diameter, perfectly matching the laser depth set. Close below the end of the vertical laser cut, the stromal collagen fibrillae were regular shaped, and adjacent Descemet's

Investigative Ophthalmology & Visual Science

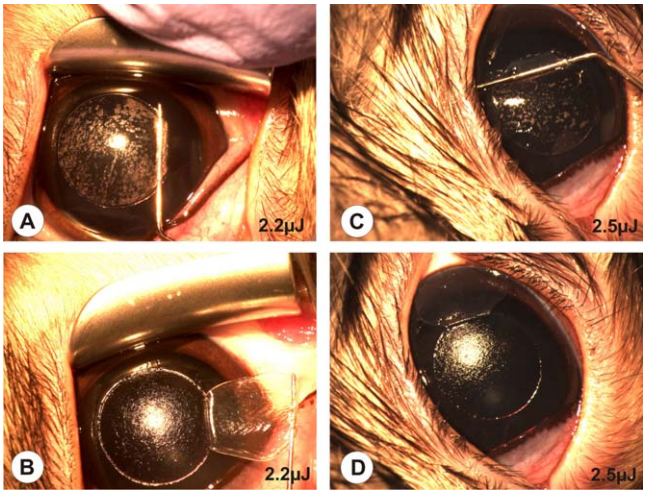


**Figure 2.** Flap lifting after corneal laser treatment at 2.2 µJ (**A**, **B**) and 2.5 µJ (**C**, **D**) and a spot distance of 6 × 6 µm. The dissection plane could be easily opened and the flap could be fully detached, showing a homogenous stromal bed with both energies used (**B**, **D**).

membrane as well as endothelium were intact without any signs of impairment. The region of the horizontal cut impressed as an acellular band of approximately 30 µm (for detailed analysis see "TUNEL assay" below), sometimes displaying a rope–ladder pattern, which facilitated the detection of the horizontal cut (Fig. 3B). No obvious differences between the effects produced by the two laser energies were found (Figs. 3B, 3D).

## Corneal Thickness

Twenty-four hours after laser treatment, a significant increase in corneal thickness was detected in 10 of 15 evaluated corneas (4 of 6 at 2.2 µJ; 6 of 9 at 2.5 µJ) when the horizontal cut region was compared with adjacent untreated cornea.

The average increase in corneal thickness of corneas treated with different laser energies did not differ significantly (2.2 µJ: 60.17 µm SD: 59.61; 2.5 µJ: 34.31 µm SD: 38.02, $P = 0.320$).

## TUNEL Assay

TdT-dUTP terminal nick-end labeling assay revealed apoptotic and necrotic cells in the horizontal as well as in the vertical cut at 6- and 12-hours post laser treatment (Figs. 4A, 4B). At 24-hours post treatment, apoptotic/necrotic cells were mainly detectable in the horizontal cut (Figs. 4C, 4D), while few TUNEL-positive cells were found in the most superficial epithelial layers (Figs. 4E, 4F). TdT-dUTP terminal nick-end labeling–positive cells were never observed in any part of the endothelium.

The amount of TUNEL-positive cells in the ROI around the horizontal cut remained stable at 6-, 12-, and 24-hours postlaser treatment when 2.2-µJ energy was applied (Table 2, different time points, one-way ANOVA, $P = 0.063$). This evaluation was not performed for 2.5 µJ.

At 24 hours (Table 2, different laser energies), no significant difference in the increase of TUNEL-positive cells within the ROI was observed between the two laser energies (2.2 µJ: 13.79% ± 9.64% [89.04 ± 49.99 TUNEL-positive cells/mm$^2$, 732.87 ± 378.06 DAPI-positive cells/mm$^2$] vs. 2.5 µJ: 14.09% ± 7.03%; [189.77 ± 91.41 TUNEL-positive cells/mm$^2$, 1384.95 ± 281.09 DAPI-positive cells/mm$^2$] $P = 0.9$). By contrast the width of the hypocellular region was significantly smaller for 2.2 µJ than for 2.5 µJ (28.07 ± 8.5 µm vs. 35.81 ± 10.71 µm; $P = 0.007$). However, no significant difference was found when the width of the hypocellular region was related to the total corneal thickness. The fraction of the hypocellular layer was 8.41% ± 1.48 for an energy of 2.2 µJ, and 10.88% ± 2.39 for 2.5 µJ, $P = 0.060$.

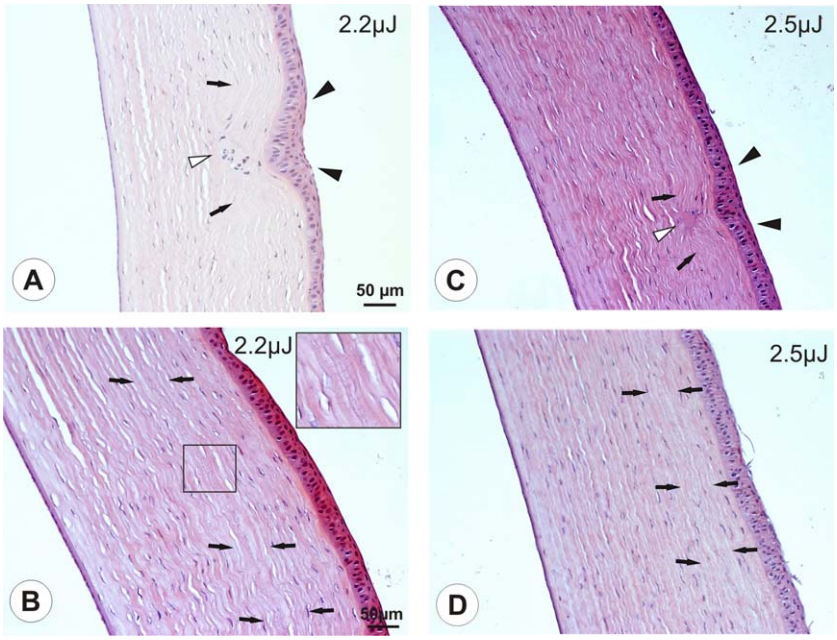


**Figure 3.** Hematoxylin and eosin–stained corneal sections after laser treatment with 2.2 µJ (**A**, **B**) and 2.5 µJ (**C**, **D**). At the location of the side cuts a dip-like thickening of the epithelium reaching into the stroma (*arrowheads*) is observed with disturbance of the arrangement of the underlying collagen fibers (*arrows*) and an edematous gap (*white arrowhead*), representing the vertical cut. In the region of the horizontal cut, a belt-like area lacking stromal keratinocytes was detected ([**B**, **D**]; *arrows*). Often, vertical stripes were detectable at the site of the horizontal cut, making its identification possible (*inset*, [**B**]). Endothelium and epithelium are intact (light microscopy, standard HE staining).

Investigative Ophthalmology & Visual Science

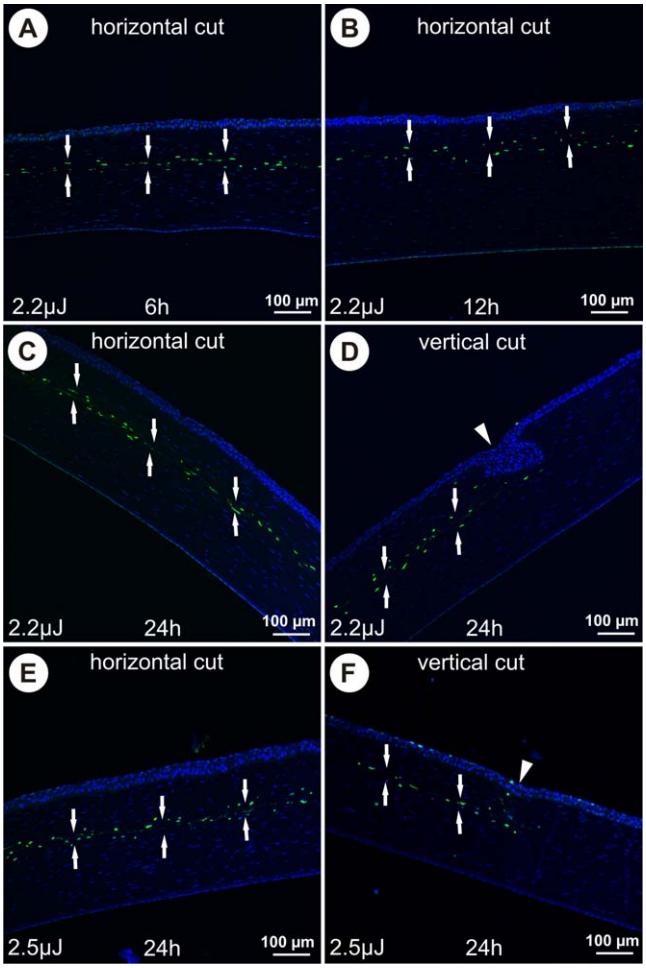


**Figure 4.** TdT-dUTP terminal nick-end labeling–positive cells (*green*) in laser-treated corneas: at 2.2 µJ, the amount of TUNEL-positive cells remained stable at different times ([**A**–**D**]; *arrows*) in the horizontal region, while in the vertical cut region ([**D**], *arrowhead*) TUNEL-positive cells were sparse. At 24-hours posttreatment, the horizontal cut did not significantly differ between 2.5 and 2.2 µJ ([**E**, **F**]; *arrows*), as it was the case in the vertical cut region ([**F**]; *arrowhead*). All figures are confocal images in single optical section mode; *blue*, DAPI.

### Transmission Electron Microscopy

At the site of the epithelial dip above the vertical cut collagen lamellae of the stroma were disrupted (Fig. 5A) or indented (Fig. 6A), forming a concavity of around 50 µm, filled with epithelial cells (Figs. 5A, 5B, 6A, 6B). Twenty-four hours after laser treatment, these epithelial cells were regularly arranged, with proper cell–cell contacts forming hemidesmosomes (Figs. 5C, 5D, 6C, 6D, 6E). At the bottom of the epithelial dip, the border to the stroma was intact over a wide range, but appeared disorganized at some places (Fig. 5E). Closely below the laser depth set, stromal collagen fibers as well as stromal keratinocytes were unaltered (Figs. 5F, 6F). The border to Descemet's membrane was intact and unaltered, as was the border from Descemet's membrane to the endothelium (Figs. 5G, 6G). Endothelial cells were regularly arranged and shaped with proper cell–cell connections, and cell organelles (endoplasmic reticulum, mitochondria) were regularly organized and without alterations (Figs. 5H, 5I, 6H, 6I). With respect to size and number, endothelial vacuoles in treated corneas resembled those in untreated control tissues.

The horizontal cutting bed appeared as a zone of disorganization of the collagen fibrils, of approximately 10-µm thickness for both laser energies (Figs. 7A, 7C). Close to this disorganization zone, the tissue was unaltered (Figs. 7B, 7D). At 2.5 µJ the cut was more clearly visible, and more electron-dense material was detectable at the cutting edge (Fig. 7D). The rope–ladder pattern observed in the HE-stained sections was not detectable at the ultrastructural level.

## Discussion

In the present study, we tested a new nanosecond UV laser (355 nm) for its feasibility in corneal surgery. Flap cuts such as in LASIK were produced at two different laser pulse energies: 2.2 µJ (6.1 J/cm$^2$, 6 × 6 µm spot distance) and 2.5 µJ (6.9 J/cm$^2$, 6 × 6 µm spot distance) in an acute animal model. Corneal tissue was processed for histology, TUNEL assay, and ultrastructural analysis to investigate possible thermomechanical and photochemical damage of the corneal tissue.

### Flap Creation

The standard protocol for corneal flap creation uses femtosecond lasers operating in near infrared at 1053 nm. Earlier studies using a femtosecond UV laser at 345 nm also resulted in successful flap creation and were performed in porcine eyes.[10] However, these studies used enucleated eyes, and the results provide limited insight into physiological tissue behavior. In the present study corneal flap creation was successful at both energy levels set, however, removal of the flap was easier at 2.5 µJ. The lower energy level (2.2 µJ) provided enough energy to lift the flap, but adherence of the stromal fibers required more force than in common clinical practice to separate the flap from the underlying tissue.

### UV Light and Safety Considerations

Since UV light can cause considerable damage to living tissue,[11] certain restrictions apply when used in routine operations. The actual risk potential depends both on the wavelength and the

**Table 2.** Evaluation of TUNEL-Positive Cells in the Horizontal Cut

| Time Point | Energy | Spot Distance | Mean # TUNEL-Positive Cells/mm$^2$ | SD mean # TUNEL-Positive Cells/mm$^2$ | Mean % TUNEL-Positive Cells/mm$^2$ | SD mean % TUNEL-Positive Cells/mm$^2$ | Statistics |
|---|---|---|---|---|---|---|---|
| Different time points | | | | | | | |
| 6 h | 2.2 µJ | 6 × 6 µm | 262.72 | 44.39 | 19.56 | 8.40 | Not significant |
| 12 h | 2.2 µJ | 6 × 6 µm | 144.16 | 56.30 | 12.26 | 4.36 | $P = 0.063$ |
| 24 h | 2.2 µJ | 6 × 6 µm | 89.04 | 49.99 | 13.79 | 9.648 | |
| Different laser energies | | | | | | | |
| 24 h | 2.2 µJ | 6 × 6 µm | 89.04 | 49.99 | 13.79 | 9.648 | Not significant |
| 24 h | 2.5 µJ | 6 × 6 µm | 189.77 | 91.41 | 14.097 | 7.037 | $P = 0.9$ |

Investigative Ophthalmology & Visual Science

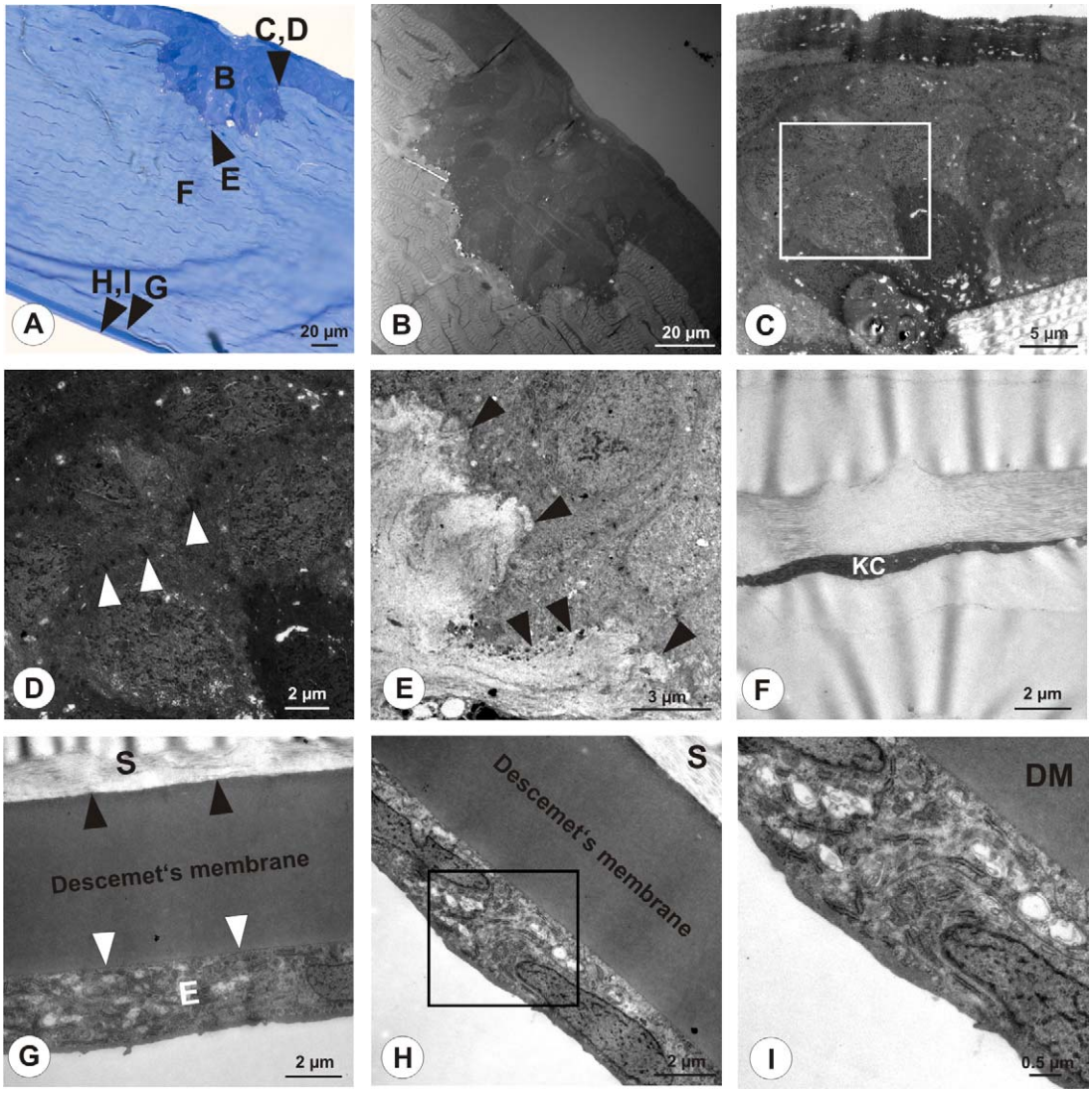


**Figure 5.** (**A**) Semithin section (toluidine blue) with marks (*letters/arrowheads*) at sites of subsequent ultrastructural analysis 24 hours after laser treatment at 2.2 µJ; (**B**) region of the vertical cut with epithelial dip. Epithelial layers display unaltered arrangement (**C**) with regular cell–cell contacts of the hemidesmosome type ([**D**], *arrowheads*; magnification of the *boxed area* in [**C**]). The transition zone epithelium–stroma appears disorganized at some places ([**E**], *arrowheads*) but is more or less intact. Directly below the vertical cut (**F**), the stromal arrangement was unaltered (KC, stromal keratinocyte). Here, (**G**) also the transition zone stroma–Descemet's membrane (*black arrowheads*) and Descemet's membrane–endothelium (*white arrowheads*) was intact (S, stroma; E, endothelium). At the same site, endothelial cells (**H**) display unaltered ultrastructural morphology (S, stroma; [**I**], magnification of *boxed area* in [**H**]).

irradiation dose applied. For the laser wavelength of 355 nm used in this study a safety threshold at 19 J/cm$^2$ for the entire eye, was set by the International Commission on Non-Ionizing Radiation Protection (ICNIRP)[12] (Fig. 8). However, for a detailed analysis of the risks of possible UV damage, various compartments of the eye need to be considered independently because the absorbance for UV light differs greatly between layers, and cellular layers are more vulnerable than acellular optical media. Several groups have studied wavelength dependence of light transmittance through the different ocular media relevant for ocular safety considerations.[13,14]

Figure 9A demonstrates that corneal light transmittance at 355 nm is around 70%, which means that the laser pulses can easily reach the depth at which the flap is cut. However, approximately one-third of the energy is absorbed within the cornea, and is thus a potential source of photochemical damage.

The threshold of UV damage to the corneal epithelium has been reviewed[15,16] and it has been shown that UV-A wavelengths (380–315 nm) are considerably less hazardous than light from the UV-B (315–280 nm) and UV-C (<280 nm) regions.

The corneal epithelium in humans, monkeys, and rabbits shows a peak sensitivity to UV radiation at 270 nm[17,18] (Fig. 8[12,15]), while the threshold at 355 nm amounts to 42 J/cm,[2,15] which is approximately four orders of magnitude higher than at 270 nm. These data suggest that no photochemical damage is to be expected when flap dissection is performed at radiant exposures of 6.1 and 6.9 J/cm$^2$. Corneal UV light exposure in the present study is thus well within the safety limits suggested by others.[19] However, one needs to consider that the corneal UV radiation threshold for photokeratitis in pigmented rabbits of 42.5 J/cm$^2$ (at 365 nm)[15,19] was determined for pure UV light exposure. In flap cutting, a combination of UV damage and thermomechanical stress has to be considered. The occurrence of shock waves and cavitation bubbles resulting from plasma formation, together with the UV exposure might

Investigative Ophthalmology & Visual Science

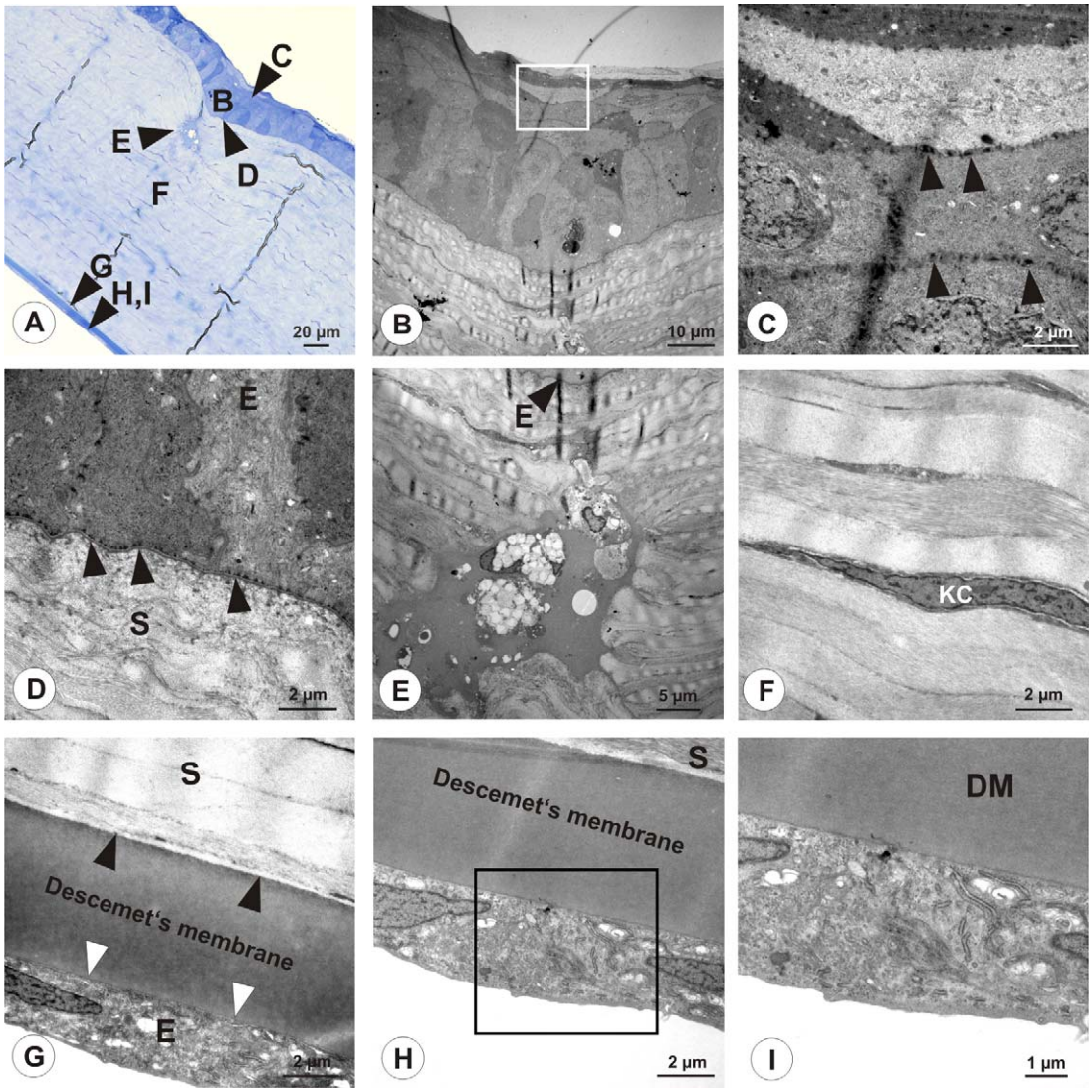


**Figure 6.** (**A**) Semithin section (toluidine blue) with marks (*letters/arrowheads*) at sites of subsequent ultra structural analysis 24 hours after laser treatment at 2.5 µJ. (**B**) Region of the vertical cut with epithelial dip (*boxed area* magnified in [**C**]). Epithelial layers display unaltered arrangement with regular cell–cell contacts of the hemidesmosome type (*arrowheads* in [**C**]). (**D**) The transition zone epithelium–stroma is intact with unaltered cell contacts to the basement membrane (hemidesmosomes, *arrowheads*; E, epithelium; S, stroma). At the stromal site of the vertical cut (**E**), the laser formed a cavity filled with amorphous material and lymph-like precipitates. Directly below the vertical cut (**F**), the stromal arrangement was unaltered (KC, stromal keratinocyte). (**G**) The transition zones stroma–Descemet's membrane (*black arrowheads*) and Descemet's membrane–endothelium (*white arrowheads*) were intact (S, stroma, E, endothelium). At the same site, endothelial cells (**H**) display unaltered ultrastructural morphology (S, stroma; [**I**], magnification of *boxed area* in [**H**]; DM, Descemet's membrane).

lead to negative synergistic effects within the target tissue.[20] Nevertheless, apart from keratocyte cell death in the stromal cutting region, which was comparable with keratocyte cell death after LASIK treatment at 1053 nm, no damage was detected in the corneal epithelium or endothelium with the laser energies used at 355 nm.

Since most of the UV light at wavelengths above 295 nm is transmitted through the cornea,[21,22] long time exposure to UV-B radiation leads to an increased risk of cataract formation.[23] Furthermore, the laser wavelength used for the present study (355 nm) is partially transmitted through the lens and may also have the potential to cause damage to the retina. To calculate the transmittance of the light incident at the cornea toward the posterior eye, van de Norren and van de Kraats[24] introduced mean density and aging coefficients, allowing to determine ocular transmittance in an age and wavelength dependent way. In Figure 9C, ocular transmittance at 355 nm is presented for different ages. For a 20-year-old eye, it was calculated to be less than 0.1% meaning less than 0.1% of the applied light at the cornea will reach the retina, and it further declines with age. These calculation results are in good concordance with experimental data obtained by Boettner[13] and Maher.[14] The thresholds for lens and retinal damage at 355 nm were not investigated in the acute experiment design of the present study. Further studies to address these questions are pending. However, considering the fact that less than 0.1% of the laser light reaches the ocular fundus, and that in flap cutting the retinal dose is spread over a large area well exceeding 1 $cm^2$, retinal damage is very unlikely.

## Epithelium

Subablative supratreshold exposure at 193 nm in rabbits led to superficial epithelial haze[25] that disappeared within several

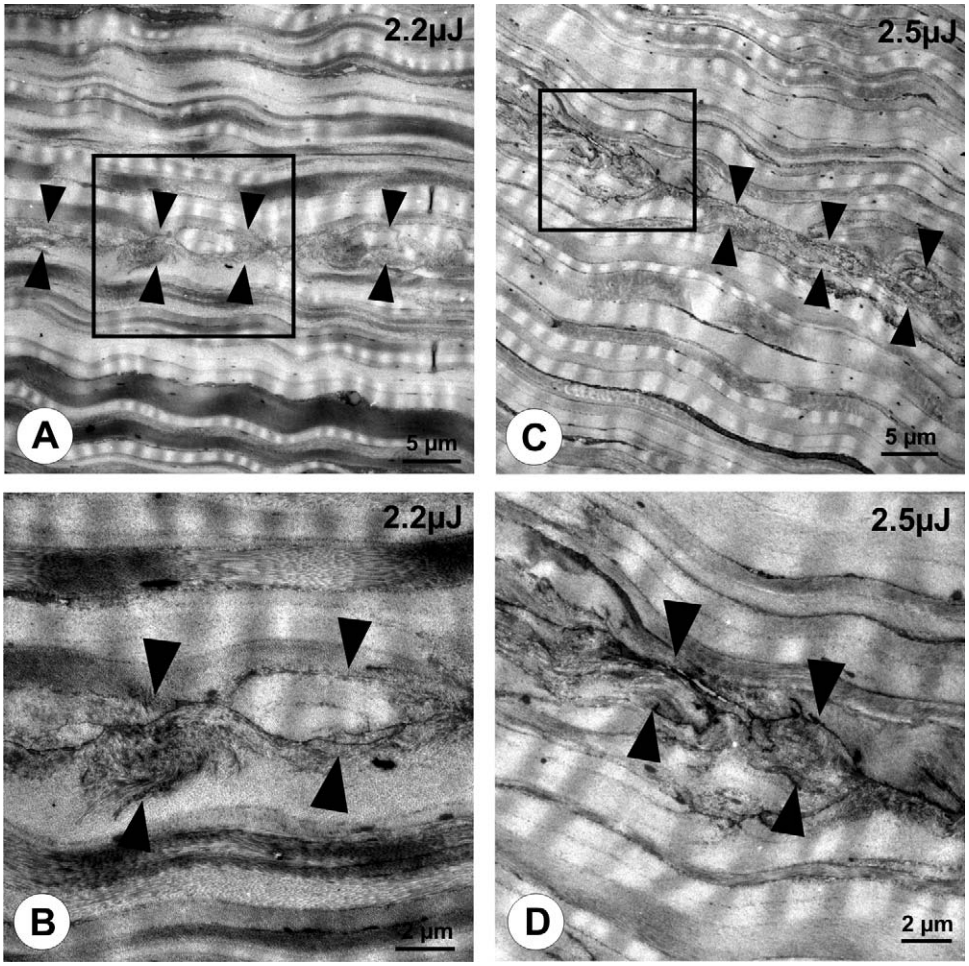


**Figure 7.** Horizontal cut at 2.2 µJ (**A**, **B**) and 2.5 µJ (**C**, **D**) at the ultrastructural level: a band like disorganization in the shape of collagen lamellae was observed (*arrowheads* in [**A**, **C**]) with intermittent bleb-like structures (*arrowheads* [**B**, **D**]). At 2.5 µJ, more electron-dense material was detectable at the cutting edge and it appeared more prominent ([**B**, **D**] represent magnified views of the *boxed areas* in [**A**, **C**]).

hours after treatment. Exposure to 312 nm in chronic experiments led to loss of corneal transparency and subsequent inflammation.[26] A loss of epithelial cells in corneas treated at 280 and 310 nm 24-hours posttreatment has been reported.[27] Such results were never observed in our set of experiments 24 hours after treatment. Further, corneal granules reported after treatment[15] were absent in retroillumination. These observations could be confirmed using standard histology: besides an epithelial dip at the site of the vertical cut, the tissue appeared normal and further, at the ultrastruc-

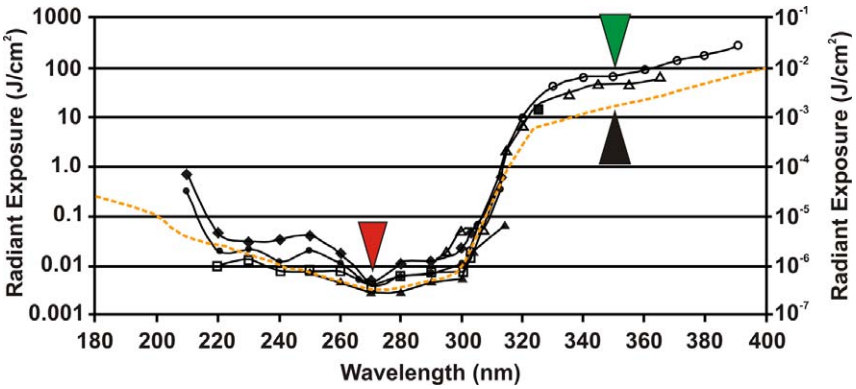


**Figure 8.** Plot of UV action spectra. Modified and reprinted with permission from Matthes. McKinlay AF, Bernhardt JH, Ahlbom A, et al. Guidelines on limits of exposure to ultraviolet radiation of wavelengths between 180 nm and 400 nm (incoherent optical radiation). *Health Phys*. 2004;87:171–186. Copyright 2004 Health Physics Society. Corneal epithelium of human, monkey, and rabbit shows a maximum sensitivity at 270 nm (*red arrowhead*), while at 355 nm the threshold is four orders of magnitude higher and amounts to 42 J/cm² (*green arrowhead*). The ICNIRP[12] defined a safety threshold of 19 J/cm² for UV radiation at 355 nm for the entire eye (*orange dotted line*). Laser energy used during our cutting procedure (6.1 and 6.9 µJ) is approximately 60% below the safety threshold defined by ICNIRP (*black arrowhead*).

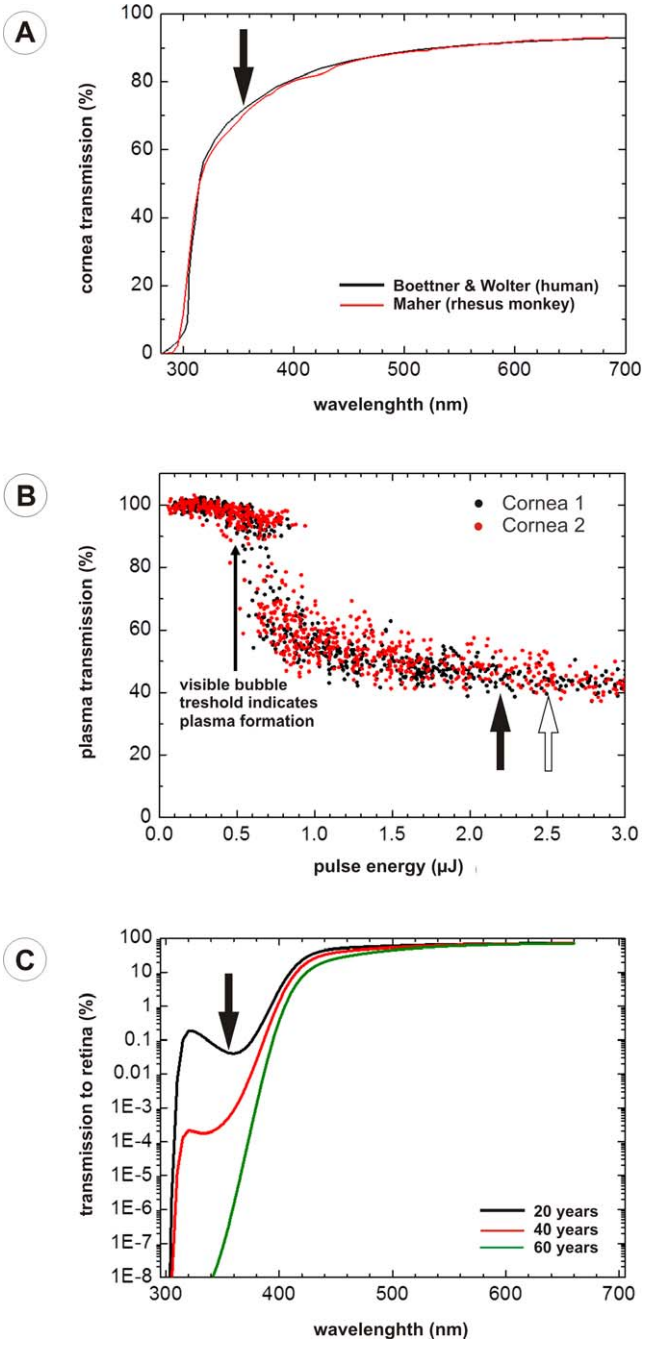


**Figure 9.** (**A**) Corneal transmission at different wavelengths in human and rhesus monkey, according to experimental data of Boettner and Wolter[13] and Maher[14] at 355 nm (*black arrow*), 70% of the light is transmitted through the cornea, while 30% of UV radiation is absorbed within corneal tissue. (**B**) Transmittance of UV laser pulses of 355 nm wavelength through porcine cornea as a function of pulse energy, for the energies used for flap cutting plasma is generated, which absorbs 54% (at 2.2 µJ, *black arrow*) and 56% (at 2.5 µJ; *white arrow*) of the incident UV light. (**C**) Transmission of UV radiation toward the retina, calculated with the help of mean density and aging coefficients, introduced by van de Kraats and van de Norren.[24] These coefficients allow to determine average data for the age and wavelength dependence of ocular transmittance. At 355 nm (*black arrow*), less than 0.1% of the applied light at the cornea will reach the retina in a 20-year-old eye, and this fraction further declines with age.

tural level, the superficial epithelial wingcells were mainly unaltered.[15] As a consequence, it can be concluded that photokeratitis as a sign of acute UV damage[28] did not occur in the present experiments. This is attributed to the strongly elevated damage thresholds at 355 nm, which are three orders of magnitude higher than in the wavelength range between 220 and 310 nm (Fig. 8).

## Endothelium

Acute suprathreshold UV-B irradiation (290–320 nm) induces endothelial cell damage leading to the formation of vacuoles,[15] blebs,[29] and disorganized cell borders,[29] eventually resulting in corneal swelling.[30] In rabbits, cell density after UV-B exposure remained without detectable pathology,[31] and also the cell density of endothelial cells in acute human UV keratitis remained unaltered after UV exposure slightly above the damage threshold.[32] Nevertheless, apoptotic endothelial cells have been reported in supratreshold rabbit experiments at 310 nm.[27] In our set of experiments, we never observed any of those altered parameters with the different energies applied, neither in standard histology nor at the ultrastructural level.

These findings are also supported by our transmission studies in porcine cadaver corneas (Fig. 9B), revealing a plasma transmittance during flap creation of approximately 46% at 2.2 µJ, and approximately 44%, at 2.5 µJ laser pulse energy. In this case, the corresponding values for the total corneal transmission to the endothelium are given by the product of plasma transmittance and corneal transmittance without plasma formation (Fig. 9B). They account for 33% at 2.2 µJ and 31% at 2.5 µJ laser pulse energy, respectively. Thus, the transmission of UV radiation to the corneal endothelium is reduced during the cutting procedure, and therefore the risk of endothelial damage is smaller than in procedures lacking plasma formation, such as corneal cross-linking. In summary, acute UV damage of the endothelium did not occur in the present study.

## Corneal Stroma

After 24 hours, supratreshold UV radiation (310 nm) in rabbits leads to apoptosis of stromal keratinocytes, followed by a loss of keratinocytes in central corneas.[27] At shorter UV range (280 nm) only superficial keratinocytes are affected because of the shallow penetration depth into the cornea (Fig. 9A). By contrast, a deep and extensive stromal damage has been reported for 310 nm, showing TUNEL signal "in almost all keratocytes in the entire thickness of the corneal stroma."[27] In our set of experiments, only a small acellular region with approximately 30 µm thickness in diameter was detectable 24 hours after laser treatment, corresponding to the horizontal cut region, and this damage appears to be less severe than reported earlier for 310 nm. A lack of keratinocytes after supratreshold UV-exposure at 310 nm shows repopulation within 7 days,[33] and also corneal cross-linking experiments revealed, that a loss of keratinocytes after UV-light exposure is a reversible process.[34–36] The number of TUNEL-positive cells in the central and peripheral cornea 24 hours after microkeratome and femtosecond laser treatment (1053 nm) was investigated in several studies.[37–39] Remarkable is, that when comparing the number of TUNEL-positive cells in the cornea after treatment with the new nanosecond laser to those observed after femtosecond laser treatment, the number of TUNEL-positive cells in our experiment appears to be lower (at 355 nm and 150 KHz: mean: 189.77 cells/mm$^2$, SD: 91.41 with 2.5 µJ, 6 × 6 µm spot distance; at 1053 nm and 60 kHz: 12.3 cells per ×400 field,[37] which corresponds approximately to 268 cells/mm$^2$ SE: 23 when recalculated).

Investigative Ophthalmology & Visual Science

The loss of keratinocytes in the horizontal cut region of the stroma observed with the infrared femtosecond laser cannot be related to UV damage, but must be caused by the thermomechanical action of plasma-induced shock waves and cavitation. Since the keratinocyte loss caused by the UV laser is lower or at least equivalent to the available infrared data, we conclude that this loss is also related to mechanical damage rather than being a result of UV damage.

### Corneal Thickness

In order to keep the corneal surface untouched for subsequent ultrastructural analysis, we resisted to perform pachymetry after laser treatment. Instead, direct measurements of corneal thickness were performed on histologic slides. This also circumvents problems in tissue shrinkage during fixation[40] compared with pachymetry values, but enables for direct comparison of different corneal regions, since central and peripheral corneal thickness in rabbits are identical.[8,9]

Acute suprathreshold UV-B irradiation leads to damage of the corneal epi- and endothelium,[41] which, besides pain,[42] results in altered corneal deturgescence due to a mismatch in hydration. This hydration mismatch, in turn, causes corneal swelling and haze. In earlier experiments of corneal UV-B irradiation at 312 nm, a dose-dependent increase in corneal thickness was observed 24 hours after irradiation (0.25 J/cm$^2$: ~8%[43]; 0.5 J/cm$^2$: ~35%[44]; 0.5 J/cm$^2$: ~65%[45]; 1.01 J/cm$^2$: ~150%[45]). Here, the onset of a thickness increase occurred at a dose of 0.25 J/cm$^2$, which is approximately twice the corneal damage threshold at 312 nm (Fig. 8). Although a significant increase in corneal thickness was observed also in our set of experiments (mean 16.6% and 9.4%, for both energy levels, respectively) this increase was much lower compared with aforementioned studies, albeit the total energies used in our study were much higher (6.1 and 6.9 J/cm$^2$, respectively). This is consistent with the higher damage threshold of 42.5 J/cm$^2$ reported for 355 nm, which exceed the applied laser dose by a factor of 6 to 7. Since also no significant differences regarding corneal swelling between both energy levels were obvious and further taking into account that corneal haze was never observed in our studies, a serious corneal damage can be denied.

## Conclusions

This new UV nanosecond laser revealed no epi- nor endothelial damage in the rabbit cornea at the laser energies feasible for cutting corneal flaps. The corneal stroma showed loss of keratinocytes in the horizontal cutting bed similar to infrared femtosecond laser systems. Pending studies will address effects of the UV nanosecond laser on the cornea, lens, and retina in chronic models.

### *Acknowledgments*

Supported by grants from the Austrian Academy of Sciences (DOC 22926, DOCf 22956), Paracelsus Medical University (FFF R09/01/001-REI), Fuchs Foundation for Research in Ophthalmology (G27), The Lotte Schwarz Endowment for Experimental Ophthalmology and Glaucoma Research, The Adele-Rabensteiner Foundation of the Austrian Ophthalmological Society, and an institutional grant from the Department of Ophthalmology Salzburg.

Disclosure: **A. Trost**, None; **F. Schrödl**, None; **C. Strohmaier**, None; **B. Bogner**, None; **C. Runge**, None; **A. Kaser-Eichberger**, None; **K. Krefft**, None; **A. Vogel**, None; **N. Linz**, None; **S. Freidank**, None; **A. Hilpert**, None; **I. Zimmermann**, None; **G. Grabner**, None; **H.A. Reitsamer**, None

### *References*

1. McAlinden C. Corneal refractive surgery: past to present. *Clin Exp Optom*. 2012;95:386–398.
2. Trokel SL, Srinivasan R, Braren B. Excimer laser surgery of the cornea. *Am J Ophthalmol*. 1983;96:710–715.
3. Kymionis GD, Kankariya VP, Plaka AD, Reinstein DZ. Femtosecond laser technology in corneal refractive surgery: a review. *J Refract Surg*. 2012;28:912–920.
4. Soong HK, Malta JB. Femtosecond lasers in ophthalmology. *Am J Ophthalmol*. 2009;147:189–197, e182.
5. Juhasz T, Loesel F, Kurtz R, Horvath C, Bille J, Mourou G. Corneal refractive surgery with femtosecond lasers. *IEEE J Sel Topics Quantum Electron*. 1999;5:902–910.
6. Vogel A, Linz N, Freidank S, inventors; Universität zu Lubeck, assignee. Method for Laser Machining Transparent Materials. US patent 8,350,183 B2. January 8, 2013.
7. Vogel A, Linz N, Freidank S, Faust S, Schwed S. LASIK-flaperzeugung mit UV-subnanosekundenpulsen. *Der Augenspiegel*. 2011;12:18–21.
8. Chan T, Payor S, Holden BA. Corneal thickness profiles in rabbits using an ultrasonic pachometer. *Invest Ophthalmol Vis Sci*. 1983;24:1408–1410.
9. Wang X, Wu Q. Normal corneal thickness measurements in pigmented rabbits using spectral-domain anterior segment optical coherence tomography. *Vet Ophthalmol*. 2012;16:130–134.
10. Le Harzic R, Konig K, Wullner C, Vogler K, Dnitzky C. Ultraviolet femtosecond laser creation of corneal flap. *J Refract Surg*. 2009;25:383–389.
11. Coohill TP. Uses and effects of ultraviolet radiation on cells and tissues. In: Waynant RW, ed. *Lasers in Medicine*. Boca Raton, FL: CRC Press; 2002:85–107.
12. McKinlay AF, Bernhardt JH, Ahlbom A, et al. Guidelines on limits of exposure to ultraviolet radiation of wavelengths between 180 nm and 400 nm (incoherent optical radiation). *Health Phys*. 2004;87:171–186.
13. Boettner EA, Wolter R. Transmission of the ocular media. *Invest Ophthalmol Vis Sci*. 1962;1:776–783.
14. Maher E. Transmission and absorption coefficients for ocular media of the Rhesus monkey. *Report SAM-TR-78-32, USAF School of Aerospace Medicine, Brooks AFB, Texas*. 1978. Available at: http://www.dtic.mil/dtic/tr/fulltext/u2/a064868.pdf. Accessed November 16, 2013.
15. Cullen AP. Photokeratitis and other phototoxic effects on the cornea and conjunctiva. *Int J Toxicol*. 2002;21:455–464.
16. Chaney EK, Sliney DH. Re-evaluation of the ultraviolet hazard action spectrum–the impact of spectral bandwidth. *Health Phys*. 2005;89:322–332.
17. Pitts DG, Tredici TJ. Effects of ultraviolet on Eye. *American Indust Hyg Assoc J*. 1971;32:235–246.
18. Kurtin WE, Zuclich JA. Action spectrum for oxygen-dependent near-ultraviolet induced corneal damage. *Photochem Photobiol*. 1978;27:329–333.
19. Pitts DG, Cullen AP, Hacker PD. Ocular effects of ultraviolet radiation from 295 to 365 nm. *Invest Ophthalmol Vis Sci*. 1977;16:932–939.
20. Vogel A, Busch S, Parlitz U. Shock wave emission and cavitation bubble generation by picosecond and nanosecond optical breakdown in water. *J Acoust Soc Am*. 1996;100:148–165.
21. Karai I, Matsumura S, Takise S, Horiguchi S, Matsuda M. Morphological change in the corneal endothelium due to ultraviolet radiation in welders. *Br J Ophthalmol*. 1984;68:544–548.

22. Zigman S. Ocular light damage. *Photochem Photobiol*. 1993; 57:1060–1068.
23. Taylor HR, West SK, Rosenthal FS, et al. Effect of ultraviolet radiation on cataract formation. *N Engl J Med*. 1988;319:1429–1433.
24. van de Kraats J, van Norren D. Optical density of the aging human ocular media in the visible and the UV. *J Opt Soc Am A Opt Image Sci Vis*. 2007;24:1842–1857.
25. Krueger RR, Sliney DH, Trokel SL. Photokeratitis from subablative 193-nanometer excimer laser radiation. *Refract Corneal Surg*. 1992;8:274–279.
26. Cejkova J, Lojda Z. The damaging effect of UV rays below 320 nm on the rabbit anterior eye segment. II. Enzyme histochemical changes and plasmin activity after prolonged irradiation, *Acta Histochem*. 1995;97:183–188.
27. Podskochy A, Gan L, Fagerholm P. Apoptosis in UV-exposed rabbit corneas. *Cornea*. 2000;19:99–103.
28. Fris M, Tessem MB, Cejkova J, Midelfart A. The effect of single and repeated UVB radiation on rabbit cornea. *Graefes Arch Clin Exp Ophthalmol*. 2006;244:1680–1687.
29. Riley MV, Susan S, Peters MI, Schwartz CA. The effects of UV-B irradiation on the corneal endothelium. *Curr Eye Res*. 1987;6: 1021–1033.
30. Cullen AP, Chou BR, Hall MG, Jany SE. Ultraviolet-B damages corneal endothelium. *Am J Optom Physiol Opt*. 1984;61:473–478.
31. Nagy ZZ, Hiscott P, Seitz B, Schlotzer-Schrehardt U, Suveges I, Naumann GO. Clinical and morphological response to UV-B irradiation after excimer laser photorefractive keratectomy. *Surv Ophthalmol*. 1997;42(suppl 1):S64–S76.
32. Najjar DM, Awwad ST, Zein WM, Haddad WF. Assessment of the corneal endothelium in acute ultraviolet keratitis. *Med Sci Monit*. 2006;12:MT23–MT25.
33. Podskochy A, Fagerholm P. Cellular response and reactive hyaluronan production in UV-exposed rabbit corneas. *Cornea*. 1998;17:640–645.
34. Kymionis GD, Diakonis VF, Kalyvianaki M, et al. One-year follow-up of corneal confocal microscopy after corneal cross-linking in patients with post laser in situ keratosmileusis ectasia and keratoconus. *Am J Ophthalmol*. 2009;147:774–778, 778 e771.
35. Mazzotta C, Balestrazzi A, Traversi C, et al. Treatment of progressive keratoconus by riboflavin-UVA-induced cross-linking of corneal collagen: ultrastructural analysis by Heidelberg Retinal Tomograph II in vivo confocal microscopy in humans. *Cornea*. 2007;26:390–397.
36. Wollensak G, Iomdina E, Dittert DD, Herbst H. Wound healing in the rabbit cornea after corneal collagen cross-linking with riboflavin and UVA. *Cornea*. 2007;26:600–605.
37. Netto MV, Mohan RR, Medeiros FW, et al. Femtosecond laser and microkeratome corneal flaps: comparison of stromal wound healing and inflammation. *J Refract Surg*. 2007;23: 667–676.
38. de Medeiros FW, Kaur H, Agrawal V, et al. Effect of femtosecond laser energy level on corneal stromal cell death and inflammation. *J Refract Surg*. 2009;25:869–874.
39. Mohan RR, Hutcheon AE, Choi R, et al. Apoptosis, necrosis, proliferation, and myofibroblast generation in the stroma following LASIK and PRK. *Exp Eye Res*. 2003;76:71–87.
40. Schned AR, Wheeler KJ, Hodorowski CA, et al. Tissue-shrinkage correction factor in the calculation of prostate cancer volume. *Am J Surg Pathol*. 1996;20:1501–1506.
41. Doughty MJ, Cullen AP. Long-term effects of a single dose of ultraviolet-B on albino rabbit cornea–I. In vivo analyses. *Photochem Photobiol*. 1989;49:185–196.
42. Bergmanson JP. Corneal damage in photokeratitis–why is it so painful? *Optom Vis Sci*. 1990;67:407–413.
43. Cejka C, Luyckx J, Cejkova J. Central corneal thickness considered an index of corneal hydration of the UVB irradiated rabbit cornea as influenced by UVB absorber. *Physiol Res*. 2012;61:299–306.
44. Cejka C, Luyckx J, Ardan T, et al. The effect of actinoquinol with hyaluronic acid in eye drops on the optical properties and oxidative damage of the rabbit cornea irradiated with UVB rays. *Photochem Photobiol*. 2010;86:1294–1306.
45. Cejka C, Rosina J, Sirc J, Michalek J, Brunova B, Cejkova J. The reversibility of UV-B induced alterations in optical properties of the rabbit cornea depends on dose of UV irradiation. *Photochem Photobiol*. 2012;89:474–482.